Applied Problems of Nonlinear Oscillation and Wave Theory

Izvestiya Vysshikh Uchebnykh Zavedeniy. Applied Nonlinear Dynamics. 2023;31(6)

Article DOI: 10.18500/0869-6632-003069

Kink dynamics of the sine-Gordon equation in a model with three identical attracting or repulsive impurities

E. G. Ekomasov[1], *R. V. Kudryavtsev*[1], *K. Yu. Samsonov*[2]✉, *V. N. Nazarov*[3], *D. K. Kabanov*[1]

[1]Ufa University of Science and Technology, Russia
[2]University of Tyumen, Russia
[3]Ufa Federal Research Centre of the RAS, Russia
E-mail: ekomasoveg@gmail.com, xc.89@mail.ru, ✉k.y.samsonov@gmail.com, nazarovvn@gmail.com, danya.kabanov.95@mail.ru

Received 15.05.2023, accepted 9.07.2023, available online 17.11.2023, published 30.11.2023

Abstract. *Purpose* of this work is to use analytical and numerical methods to consider the problem of the structure and dynamics of the kinks in the sine-Gordon model with "impurities" (or spatial inhomogeneity of the periodic potential). *Methods.* Using the method of collective variables for the case of three identical point impurities located at the same distance from each other, a system of differential equations is obtained. Resulting system of equations makes it possible to describe the dynamics of the kink taking into account the excitation of localized waves on impurities. To analyze the dynamics of the kink in the case of extended impurities, a numerical finite difference method with an explicit integration scheme was applied. Frequency analysis of kink oscillations and localized waves calculated numerically was performed using a discrete Fourier transform. *Results.* For the kink dynamics, taking into account the excitation of oscillations in modes, a system of equations for the coordinate of the kink center and the amplitudes of waves localized on impurities is obtained and investigated. Significant differences are observed in the dynamics of the kink when interacting with a repulsive and attractive impurity. The dynamics of the kink in a model with three identical extended impurities, taking into account possible resonant effects, was solved numerically. It is established that the found scenarios of kink dynamics for an extended rectangular impurity are qualitatively similar to the scenarios obtained for a point impurity described using a delta function. All possible scenarios of kink dynamics were determined and described taking into account resonant effects. *Conclusion.* The analysis of the influence of system parameters and initial conditions on possible scenarios of kink dynamics is carried out. Critical and resonant kink velocities are found as functions of the impurity parameters.

Keywords: sine-Gordon equation, kink, soliton, breather, method of collective coordinates, impurity.

Acknowledgements. This work was supported by Russian Foundation for Basic Research, grant No. 20-31-90048.

For citation: Ekomasov EG, Kudryavtsev RV, Samsonov KYu, Nazarov VN, Kabanov DK. Kink dynamics of the sine-Gordon equation in a model with three identical attracting or repulsive impurities. Izvestiya VUZ. Applied Nonlinear Dynamics. 2023;31(6):693–709. DOI: 10.18500/0869-6632-003069

Introduction

One of the most studied nonlinear differential equations currently belonging to the class of Klein-Gordon equations is the sine-Gordon equation [1–3]. It is used to describe wave processes in geology, molecular biology, physics, cosmology [2–4].

For example, in condensed matter physics, the sine-Gordon equation is used to describe the dynamics of magnetization waves in ferromagnetic crystals, the movement of dislocations in crystals, processes in Josephson superconducting contacts, the propagation of charge density waves in one-dimensional organic conductors, the propagation of electromagnetic waves in a graphene-based superlattice, the dynamics of an ensemble of interacting dislocations in a linear defect of the electroconvective structure of a liquid crystal [5–9].

The sine-Gordon equation is a nonlinear partial differential equation and at the same time fully integrable. Many of his exact solutions such as kink, soliton, breather and complex multisoliton type [1, 2, 10, 11] are known. Finding new solutions to the sine-Gordon equation and investigating the effects of various perturbations and modifications is an urgent task of the modern theory of nonlinear waves.

For use in real physical models, additional terms [1, 2, 12, 13] are often added to the sine-Gordon equations. These terms are needed to account for the presence of external forces and dissipation in the system, heterogeneity of environmental parameters, and so on. The sine-Gordon equation obtained as a result of this modification no longer has precise analytical solutions. In such cases, the perturbation theory for solitons or the method of collective coordinates [1,2,13–15] is often used, with the help of which it was possible to obtain solutions for a large number of similar problems. For example, the dynamics of kinks, solitons and breathers under the action of various types of external force, which is a function of time and spatial variables [16,17] is studied.

Another popular area of research is the study of the influence of spatial modulation of the periodic potential (impurity) on the dynamics of solitons of the equation синус-Гордона [13, 14, 18–30]. The sine-Gordon model with impurities (both point and extended modeled as a delta function) is applicable to describe the case of a multilayer ferromagnet [31–33]. The kink-impurity interaction can lead to the generation of waves localized on attracting impurities (or an impurity mode) [2, 23–30] and as a result— to a significant change in the dynamics of the kink. The attracting admixture can also lead to the excitation of the multisolitons of the sine-Gordon equation.

The case of two impurities [29, 33] provides a wide variety of new multisoliton solutions and dynamic effects compared to the case of a single impurity. We can expect an even greater variety of solutions and effects in the presence of three or more impurities in the system. In this paper, we study the dynamics of kink in a model with three identical impurities, taking into account the excitation of nonlinear waves localized on impurities.

1. Point impurity

Consider a system defined by a Lagrangian

$$L = \int\limits_{-\infty}^{\infty} \left[\frac{1}{2} u_t^2 - \frac{1}{2} u_x^2 + (1 - \varepsilon\delta(x) - \varepsilon\delta(x-d) - \varepsilon\delta(x-2d))(1 - \cos u) \right] dx, \tag{1}$$

where $\varepsilon\delta(x)$ are models a point impurity, $\delta(x)$ is the Dirac delta function, ε is a constant, d is the distance between neighboring impurities. If the parameter ε is greater than zero, then we are dealing with an attractive impurity, which is a potential pit for kink. If the parameter ε is less than zero, then we are dealing with a repulsive impurity, which is a potential barrier to kink. The Lagrangian (1) corresponds to the equation of motion for a scalar field $u(x,t)$ of the form

$$u_{tt} - u_{xx} + \sin u = [\varepsilon\delta(x) - \varepsilon\delta(x-d) - \varepsilon\delta(x-2d)]\sin u. \tag{2}$$

The equation (2) is a modified sine-Gordon equation. The perturbation terms on the right side of the equation (2) describe seven-layer ferromagnetic structures with different values of magnetic anisotropy ε in different layers [21, 23]. If the right side of the equation (2) is zero, then it has a solution in the form of a kink

$$u_0 = 4\,\mathrm{arctg}\, e^{x-X(t)} \tag{3}$$

(where $X(t)$ is the coordinate of the kink center) or a spatially localized solution of the form "resting breather" [1, 2]

$$u(x,t) = 4\,\mathrm{arctg}\left(\frac{\sqrt{1-\Omega^2}}{\Omega}\frac{\sin\Omega t}{\mathrm{ch}((x-x_0)\sqrt{1-\Omega^2})}\right), \tag{4}$$

where Ω is the frequency of the breather and x_0 is the coordinate of its center.

Let's consider the dynamics of the kink, taking into account the possible excitation of localized waves on impurities. For the theoretical analysis of the structure and dynamics of solutions to the equation (2), an approximate method of collective coordinates can be used, which was previously applied to the description of kink dynamics in a model with a single point impurity [1, 2]. The presence of localized waves on three impurities (or impurity modes) is taken into account by introducing three collective variables, $a_1 = a_1(t)$, $a_2 = a_2(t)$ and $a_3 = a_3(t)$, which are the amplitudes of these waves. The form of impurity mode expressions is similar to that used earlier for the case of a single impurity [2, 29]:

$$\begin{cases} u_1 = a_1(t)\exp(-\varepsilon|x|/2), \\ u_2 = a_2(t)\exp(-\varepsilon|x-d|/2), \\ u_3 = a_3(t)\exp(-\varepsilon|x-2d|/2). \end{cases} \tag{5}$$

In the approximation of oscillations of small amplitudes, we assume that $a_n(t) = a_{n0}\cos(\Omega t + \theta_0)$, where θ_0 is the initial phase. Solving the equation (2) in the absence of a kink for the case of a single impurity, we can obtain an expression for the frequency of the impurity mode $\Omega = \sqrt{(1-\varepsilon^2/4)}$. We will look for a general solution to the problem u in the following form:

$$u = u_0 + u_1 + u_2 + u_3. \tag{6}$$

Suppose that $\dot{X}(t)$, $a_n(t)$, $\dot{a}_n(t)$ are sufficiently small (on the order of ε), that is, impurity modes with small amplitudes are excited by a slowly moving kink. Within this approximation, we consider $u_n \ll u_0$. Then the nonlinear terms in the Lagrangian (1) can be decomposed into a Taylor series up to second-order terms by ε [2]:

$$\cos(u_0 + u_1 + u_2 + u_3) \approx \cos u_0 - \frac{(u_1+u_2+u_3)^2}{2}\cos u_0. \tag{7}$$

Substituting (6) into (1) based on the approximation (7) leads, after integration, to a new effective

Lagrangian depending on the new variables $X(t)$, $a_1(t)$, $a_2(t)$ and $a_3(t)$:

$$
\begin{aligned}
L \approx & -8 + 4\dot{X}^2(t) + \frac{\dot{a}_1^2(t)}{\varepsilon} + \frac{\dot{a}_2^2(t)}{\varepsilon} + \frac{\dot{a}_3^2(t)}{\varepsilon} + 2\left(\dot{a}_1(t)\dot{a}_2(t) + \dot{a}_2(t)\dot{a}_3(t)\right)E_1 + \\
& + 2\dot{a}_1(t)\dot{a}_3(t)E_2 + 2\varepsilon a_1(t)\Big[F_1(X(t)) + F_2(X(t))e^{-\frac{\varepsilon d}{2}} + F_3(X(t))e^{-\varepsilon d}\Big] + \\
& + 2\varepsilon a_2(t)\left[F_1(X(t)) + F_3(X(t))e^{-\frac{\varepsilon d}{2}} + F_2(X(t))\right] + \\
& + 2\varepsilon a_3(t)\left[F_1(X(t))e^{-\varepsilon d} + F_2(X(t))e^{-\frac{\varepsilon d}{2}} + F_3(X(t))\right] - \\
& - 2\varepsilon a_1^2(t)\left[\frac{\Omega_0^2}{2\varepsilon^2} + \frac{1}{2}U_1(X(t)) + \frac{1}{2}U_2(X(t))e^{-\varepsilon d} + \frac{1}{2}U_3(X(t))e^{-2\varepsilon d}\right] - \\
& - 2\varepsilon a_2^2(t)\left[\frac{\Omega_1^2}{2\varepsilon^2} + \frac{1}{2}U_1(X(t))e^{-\varepsilon d} + \frac{1}{2}U_2(X(t)) + \frac{1}{2}U_3(X(t))e^{-\varepsilon d}\right] - \\
& - 2\varepsilon a_3^2(t)\left[\frac{\Omega_0^2}{2\varepsilon^2} + \frac{1}{2}U_1(X(t))e^{-2\varepsilon d} + \frac{1}{2}U_2(X(t))e^{-\varepsilon d} + \frac{1}{2}U_3(X(t))\right] - \\
& - 2\varepsilon a_1(t)a_2(t)\left[-Y_1/2\varepsilon + U_1(X(t))e^{\frac{-\varepsilon d}{2}} + U_2(X(t))e^{\frac{-\varepsilon d}{2}} + (-1/2 + U_3(X(t)))e^{\frac{-3\varepsilon d}{2}}\right] - \\
& - 2\varepsilon a_1(t)a_3(t)\Big[-Y_2/2\varepsilon + U_1(X(t))e^{-\varepsilon d} + U_2(X(t))e^{-\varepsilon d} + U_3(X(t))e^{-\varepsilon d}\Big] - \\
& - 2\varepsilon a_2(t)a_3(t)\left[-Y_1/2\varepsilon + (-1/2 + U_1(X(t)))e^{\frac{-3\varepsilon d}{2}} + U_2(X(t))e^{\frac{-\varepsilon d}{2}} + U_3(X(t))e^{-\frac{\varepsilon d}{2}}\right] + \\
& + 2\varepsilon(U_1(X(t)) + U_2(X(t)) + U_3(X(t))).
\end{aligned}
\tag{8}
$$

Here $U_1(X(t)) = \dfrac{1}{\mathrm{ch}^2(X(t))}$, $U_2(X(t)) = \dfrac{1}{\mathrm{ch}^2(X(t)-d)}$, $U_3(X(t)) = \dfrac{1}{\mathrm{ch}^2(X(t)-2d)}$,

$F_1(X(t)) = \dfrac{\mathrm{sh}(X(t))}{\mathrm{ch}^2(X(t))}$, $F_2(X(t)) = \dfrac{\mathrm{sh}(X(t)-d)}{\mathrm{ch}^2(X(t)-d)}$, $F_3(X(t)) = \dfrac{\mathrm{sh}(X(t)-2d)}{\mathrm{ch}^2(X(t)-2d)}$,

$E_1 = \dfrac{(2+\varepsilon d)}{2\varepsilon}e^{-\frac{\varepsilon d}{2}} = \left(\dfrac{1}{\varepsilon} + \dfrac{d}{2}\right)e^{-\frac{\varepsilon d}{2}}$, $E_2 = \dfrac{(1+\varepsilon d)}{\varepsilon}e^{-\varepsilon d} = \left(\dfrac{1}{\varepsilon} + d\right)e^{-\varepsilon d}$,

$\Omega_0^2 = 1 - \dfrac{\varepsilon^2}{4} - \dfrac{\varepsilon^2}{2}e^{-\varepsilon d} - \dfrac{\varepsilon^2}{2}e^{-2\varepsilon d}$, $\Omega_1^2 = 1 - \dfrac{\varepsilon^2}{4} - \varepsilon^2 e^{-\varepsilon d}$,

$Y_1 = \varepsilon e^{-\frac{\varepsilon d}{2}} + 2\left(\dfrac{\varepsilon^2}{4} - 1\right)E_1$, $Y_2 = \varepsilon e^{-\varepsilon d} + \left(\dfrac{\varepsilon^2}{4} - 1\right)E_2$.

The equations of motion for $X(t)$, $a_1(t)$, $a_2(t)$ and $a_3(t)$ can be obtained by converting the

effective Lagrangian (8) into a system of second-order Lagrangian equations:

$$
\begin{cases}
4\ddot{X}(t) - \varepsilon(U_1' + U_2' + U_3') - \varepsilon[a_1(F_1' + F_2'e_d + F_3'e_d^2) + a_2([F_1' + F_3']e_d + F_2') + \\
\quad + a_3(F_1'e_d^2 + F_2'e_d + F_3')] + \tfrac{1}{2}\varepsilon[a_1^2(U_1' + U_2'e_d^2 + U_3'e_d^4) + a_2^2([U_1' + U_3']e_d^2 + U_2') + \\
\quad + a_3^2\left(U_1'e_d^4 + U_2'e_d^2 + U_3'\right) + 2a_1a_2(U_1'e_d + U_2'e_d + U_3'e_d^3) + 2a_1a_3(U_1' + U_2' + U_3')e_d^2 + \\
\qquad + 2a_2a_3(U_1'e_d^3 + U_2'e_d + U_3'e_d)] = 0, \\
([\ddot{a}_1 + a_1(1 - \varepsilon^2/4)][(1/\varepsilon)[1 - \varepsilon^2E_1^2] - \varepsilon[E_1^2 + E_2^2 - 2\varepsilon E_1^2E_2]] + \\
\quad + a_1[[\varepsilon[U_1 + (U_2 - 1/2)e_d^2 + (U_3 - 1/2)e_d^4]][1 - \varepsilon^2E_1^2] - \\
\quad - [\varepsilon[(U_1 + U_2 - 1/2)e_d + (U_3 - 1/2)e_d^3]]\varepsilon E_1[1 - \varepsilon E_2] - \\
\quad - [\varepsilon[(U_1 + U_2 + U_3 - 1)e_d^2]]\varepsilon[E_2 - \varepsilon E_1^2]] + a_2[[\varepsilon[(U_1 + U_2 - 1/2)e_d + (U_3 - 1/2)e_d^3]] \times \\
\quad \times [1 - \varepsilon^2E_1^2] - [\varepsilon[(U_1 + U_3 - 1)e_d^2 + U_2]]\varepsilon E_1[1 - \varepsilon E_2] - \\
\quad - [\varepsilon[(U_1 - 1/2)e_d^3 + (U_2 + U_3 - 1/2)e_d]]\varepsilon[E_2 - \varepsilon E_1^2]] + a_3[[\varepsilon[(U_1 + U_2 + U_3 - 1)e_d^2]][1 - \varepsilon^2E_1^2] - \\
\quad - [\varepsilon[(U_1 - 1/2)e_d^3 + (U_2 + U_3 - 1/2)e_d]]\varepsilon E_1[1 - \varepsilon E_2] - [\varepsilon[(U_1 - 1/2)e_d^4 + \\
\quad + (U_2 - 1/2)e_d^2 + U_3]]\varepsilon[E_2 - \varepsilon E_1^2]] - [\varepsilon[(F_1 + F_2e_d + F_3e_d^2)(1 - \varepsilon^2E_1^2) - \\
\qquad - [(F_1 + F_3)e_d + F_2]\varepsilon E_1[1 - \varepsilon E_2] - [F_1e_d^2 + F_2e_d + F_3]\varepsilon[E_2 - \varepsilon E_1^2]]]) = 0, \\
([\ddot{a}_2 + a_2(1 - \varepsilon^2/4)][(1/\varepsilon)[1 - \varepsilon^2E_2^2] - 2\varepsilon E_1^2[1 - \varepsilon E_2]] + a_1[[\varepsilon[(U_1 + U_2 - 1/2)e_d + \\
\quad + (U_3 - 1/2)e_d^3]][1 - \varepsilon^2E_2^2] - [\varepsilon[U_1 + (U_1 + 2U_2 + U_3 - 3/2)e_d^2 + (U_3 - 1/2)e_d^4]] \times \\
\quad \times \varepsilon E_1[1 - \varepsilon E_2]] + a_2[[\varepsilon[U_2 + (U_1 + U_3 - 1)e_d^2]][1 - \varepsilon^2E_2^2] - [\varepsilon[(U_1 + 2U_2 + U_3 - 1)e_d + \\
\quad + (U_1 + U_3 - 1)e_d^3]]\varepsilon E_1[1 - \varepsilon E_2]] + a_3[[\varepsilon[(U_3 + U_2 - 1/2)e_d + (U_1 - 1/2)e_d^3]][1 - \varepsilon^2E_2^2] - \\
\quad - [\varepsilon[U_3 + (U_1 + 2U_2 + U_3 - 3/2)e_d^2 + (U_1 - 1/2)e_d^4]]\varepsilon E_1[1 - \varepsilon E_2]]) - \\
\qquad - (\varepsilon([(F_1 + F_3)e_d + F_2][1 - \varepsilon^2E_2^2] - [F_1(1 + e_d^2) + 2F_2e_d + F_3(1 + e_d^2)]\varepsilon E_1[1 - \varepsilon E_2])) = 0, \\
([\ddot{a}_3 + a_3(1 - \varepsilon^2/4)][(1/\varepsilon)[1 - \varepsilon^2E_1^2] - \varepsilon[E_1^2 + E_2^2 - 2\varepsilon E_1^2E_2]] + a_1[[\varepsilon[(U_1 + U_2 + U_3 - 1)e_d^2]] \times \\
\quad \times [1 - \varepsilon^2E_1^2] - [\varepsilon[(U_1 + U_2 - 1/2)e_d + (U_3 - 1/2)e_d^3]]\varepsilon E_1[1 - \varepsilon E_2] - [\varepsilon[U_1 + (U_2 - 1/2)e_d^2 + \\
\quad + (U_3 - 1/2)e_d^4]]\varepsilon[E_2 - \varepsilon E_1^2]] + a_2[[\varepsilon[(U_1 - 1/2)e_d^3 + (U_2 + U_3 - 1/2)e_d]][1 - \varepsilon^2E_1^2] - \\
\quad - [\varepsilon[(U_1 + U_3 - 1)e_d^2 + U_2]]\varepsilon E_1[1 - \varepsilon E_2] - [\varepsilon[(U_1 + U_2 - 1/2)e_d + (U_3 - 1/2)e_d^3]]\varepsilon[E_2 - \varepsilon E_1^2]] + \\
\quad + a_3[[\varepsilon[(U_1 - 1/2)e_d^4 + (U_2 - 1/2)e_d^2 + U_3]][1 - \varepsilon^2E_1^2] - [\varepsilon[(U_1 - 1/2)e_d^3 + (U_2 + U_3 - 1/2)e_d]] \times \\
\quad \times \varepsilon E_1[1 - \varepsilon E_2] - [\varepsilon[(U_1 + U_2 + U_3 - 1)e_d^2]]\varepsilon[E_2 - \varepsilon E_1^2]]) - (\varepsilon[[F_1e_d^2 + F_2e_d + F_3][1 - \varepsilon^2E_1^2] - \\
\qquad - [(F_1 + F_3)e_d + F_2]\varepsilon E_1[1 - \varepsilon E_2] - [F_1 + F_2e_d + F_3e_d^2]\varepsilon[E_2 - \varepsilon E_1^2]]) = 0,
\end{cases}
\tag{9}
$$

where $e_d = e^{\frac{-\varepsilon d}{2}}$. From the resulting set of equations in the limiting case of $d \to \infty$, one can obtain the already known equation for the case of kink motion in a model with a single impurity [2]. At $X(t) \to \infty$ equations (9) describe the associated fluctuations of impurity modes, discussed earlier in [34].

First, let's consider the effect of three impurities on the kink dynamics for the case of a repulsive impurity in the absence of impurity modes $a_n(t) = 0$:

$$
\ddot{X}(t) + \sum_{k=1}^{3}\left(\frac{\varepsilon}{2}\frac{\mathrm{th}(X(t) - x_k)}{\mathrm{ch}^2(X(t) - x_k)}\right) = 0, \tag{10}
$$

where x_k is the coordinate of the k-th impurity. The equation (10) for the case of one and two impurities reduces to the already known equation of motion of the kink [29]. Multiplying it by

$\dot{X}(t)$ and integrating it in time, we get

$$\dot{X}^2(t) - \dot{X}^2(0) - \sum_{k=1}^{3} \left(\frac{\varepsilon}{2} \left(\frac{1}{\mathrm{ch}^2(X(t) - x_k)} - \frac{1}{\mathrm{ch}^2(X(0) - x_k)} \right) \right) = 0. \tag{11}$$

If the kink moves from a long distance $X(0) \longrightarrow -\infty$, then we can simplify the form of the equation somewhat (11):

$$\dot{X}^2(t) - \dot{X}^2(0) - \sum_{k=1}^{3} \left(\frac{\varepsilon}{2} \frac{1}{\mathrm{ch}^2(X(t) - x_k)} \right) = 0. \tag{12}$$

Using the equation (12), it is possible to find the critical rates of kink dynamics for the case of an impurity in the form of a barrier (Fig. 2). Using the system of equations (9), it is possible to find all possible scenarios of kink dynamics for the case of repulsive and attractive impurities. Suppose that at the initial moment of time $t = 0$ the kink is at a relatively large distance from the impurities, $X(0) = -10$, and then moves with an initial velocity of $\dot{X}(0)$, and there are no impurity modes $a_1(0) = \dot{a}_1(0) = a_2(0) = \dot{a}_2(0) = a_3(0) = \dot{a}_3(0) = 0$. In Fig. 1, *a*, depending on the initial velocity, the following scenarios of kink dynamics were found for the case of repulsive impurities: reflection from the first barrier at a speed less than some critical one (line *3*, velocity 0.502), passage through the first barrier and reflection from the second (line *2*, velocity 0.5035), passing through all three impurities at a speed greater than the critical one (line *1*, velocity 0.505).

In Fig. 1, *b*–*d* possible cases of kink dynamics at different values of initial velocity and distance between attracting impurities are presented. During the passage of the kink, high-amplitude localized breather-type vibrations are excited on the impurities, which significantly affect the dynamics of the kink. Firstly, a significant part of the kink's energy can be spent on arousing them. Secondly, the subsequent interaction of the kink with waves localized on attracting impurities can lead to resonant effects (for example, in the case of a single impurity, reflection from a potential well [1, 2] may be observed under certain parameters).

When the impurities are located close enough to each other, depending on the initial velocity, the following cases are found: kink passage at $v_0 = 0.27$ (curve *1*, Fig. 1, *b*), the case of quasi-tunneling at $v_0 = 0.08$ (curve *2*, Fig. 1, *b*), oscillation on three impurities followed by reflection at $v_0 = 0.09$ (curve *3*, Fig. 1, *b*), the case of resonant reflection at $v_0 = 0.24$ (curve *5*, fig. 1, *b*). A case can be distinguished for $v_0 = 0.06$: the kink can fluctuate on three impurities acting as one collective impurity for a long time (curve *4*, Fig. 1, *b*). As the distance between impurities increases, it is possible to observe kink pinning on each impurity separately and a more complex kink pinning scenario with its jump between impurities (Fig. 1, *c*). By changing the distance between the impurities, the same scenarios of kink dynamics can be obtained as for the case of a change in the initial velocity (Fig 1, *d*).

2. The case of extended impurities

For practical applications, it is necessary to consider the case of extended impurities, which is more realistic from a physical point of view. The sine-Gordon equation for the case of extended impurities has the form

$$u_{tt} - u_{xx} + K(x) \sin u = 0, \tag{13}$$

where $K(x)$ is the spatial inhomogeneity of the periodic potential. It is possible to compare the results obtained for an extended impurity with the case of point impurities. The sine-Gordon

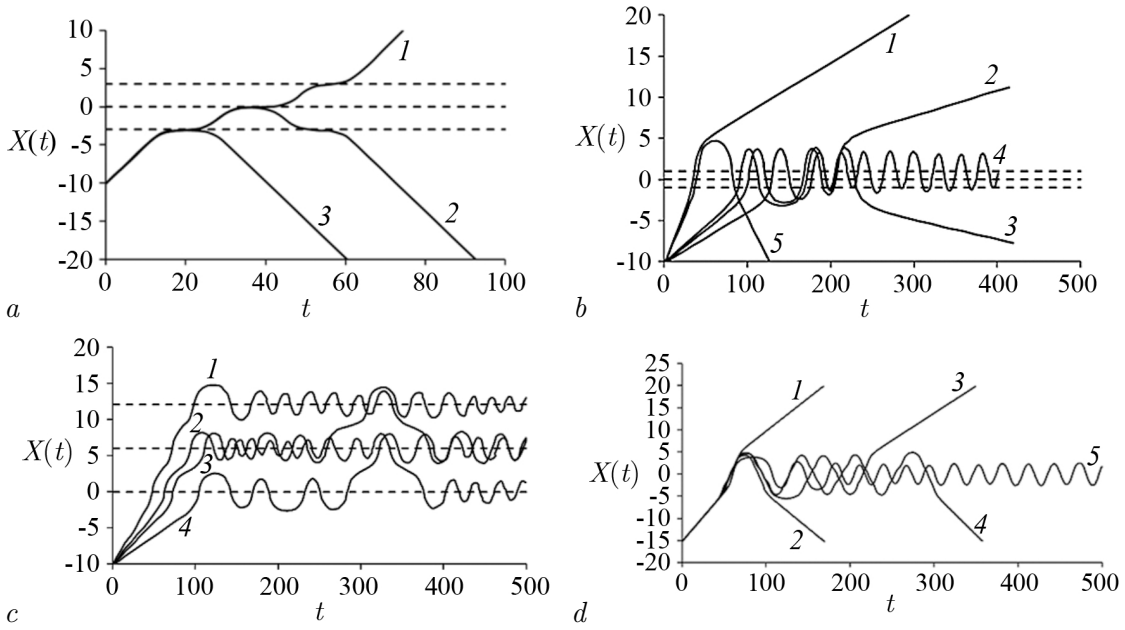

Fig 1. Dependence of the kink center coordinate X on the time t. a — The case of a barrier at $\varepsilon = -0.5$ and $d = 3$: $v_0 = 0.505$ (line *1*), $v_0 = 0.5035$ (*2*), $v_0 = 0.502$ (*3*). b — The case of a well at $d = 1$, $\varepsilon = 0.5$: $v_0 = 0.27$ (line *1*), $v_0 = 0.08$ (*2*), $v_0 = 0.09$ (*3*), $v_0 = 0.06$ (*4*), $v_0 = 0.24$ (*5*). c — The case of a well at $\varepsilon = 0.5$, $d = 6$: $v_0 = 0.188$ (line *1*), $v_0 = 0.138$ (*2*), $v_0 = 0.1165$ (*3*), $v_0 = 0.078$ (*4*). d — The case of a well at $\varepsilon = 0.5$, $v_0 = 0.22$: $d = 3.5$ (line *1*), $d = 2.5$ (*2*), $d = 2.698$ (*3*); $d = 3$ (*4*); $d = 1.2$ (*5*)

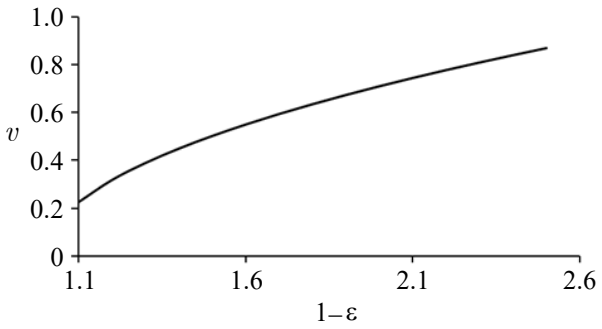

Fig 2. Dependence of the minimum speed of the kink passage over three impurities on the parameter $1 - \varepsilon$

equation in a model with extended impurities can only be solved using numerical methods. To date, a fairly large number of methods for the numerical solution of such equations have been developed [2, 14, 25, 26].

Let's use the finite difference method. Let's choose a three-layer explicit solution scheme, with approximation of derivatives on a five-point pattern of the "cross" type, which was previously used for simpler modifications of the sine-Gordon equation [24]. This is a second-order numerical scheme of approximation by Δx and τ, where Δx is a coordinate step, τ is a time step. It has conditional stability $(\tau/\Delta x) \leqslant 1/2$. In our case, the scheme is "one-step", uses a relatively small number of memory accesses and has the potential to optimize the computational algorithm.

Frequency analysis of localized wave oscillations, which are calculated numerically, is performed using a discrete Fourier transform. The fast Fourier transform algorithm is used to

calculate it. This algorithm has good performance, but the most optimized implementations of the fast Fourier transform impose certain restrictions on the original series. To prepare the data, the initial discrete dependence is interpolated by a cubic spline with natural boundary conditions, from which a new discrete dependence is constructed on a uniform grid with an increased number of approximation points. The frequency spectrum is calculated from the new discrete dependence using the fast Fourier transform. To increase the accuracy of frequency determination, the points of the maxima of the frequency spectrum are refined using interpolation by the Akim spline.

Consider the function $K(x)$ of a rectangular form:

$$K(x) = \begin{cases} 1, & \text{если } |x| > W/2, \quad |x+d| > W/2, \quad |x-d| > W/2, \\ K, & \text{если } |x| \leqslant W/2, \quad |x+d| \leqslant W/2, \quad |x-d| \leqslant W/2. \end{cases} \tag{14}$$

Let's assume that at the initial moment of time, at some distance from the impurities, there is a kink moving at a constant speed. When the kink passes through the impurity region, we investigate possible scenarios of its dynamics. Let us first consider, as in the previous paragraph, the case of the barrier. For certainty, we put the origin in the center of the second barrier. The centers of other barriers will be on both sides of it with dimensionless coordinates $x_1 = -3$ and $x_3 = 3$, $W = 1$, $K = 2$. Let the kink move from infinity towards potential barriers. We exclude the interaction of the kink with barriers at the initial moment of time. We set the initial position of the kick far enough away from the barriers.

Numerical analysis shows (Fig. 3, *a*) that the following scenarios of kink dynamics are possible: curve *1* — reflection of a kink moving at a speed of 0.59 from the first potential barrier; curve *2*— passage of a kink moving at a speed of 0.595, through the first barrier, reflection from the second and its further closed movement between the first and the second (pinning); curve *3* — passage of a kink moving at a speed of 0.59855 through the first barrier and reflection from the second; curve *4*— passage of a kink moving at a speed of 0.5986 through the first and second barriers, reflection from the third and its further closed movement between the second and third (pinning); curve *5*— passage of a kink moving at a speed of 0.602 through three barriers. The fluctuations of the kink between the first and second, between the second and third barriers are inharmonious.

For the case of an extended impurity, kink dynamics modes were found, which were obtained for point impurities in Fig. 1, as well as new modes (pinning). If we compare the values of the kink velocities before and after interaction with barriers, it turns out that these velocities are almost the same, that is, the kink-impurity interaction is almost elastic. In Fig. 4 the dependence of the minimum velocity of passage on K for the case of an extended impurity with $W = 0.5$ and 1. A comparison with the results obtained for the case of point impurities shows a qualitative coincidence of the dependencies.

Consider the case of a potential pit. In Fig. 5 shows possible scenarios of kink dynamics for the case of $K = 0.5$, $W = 1$, $d = 2$. In Fig. 5, *a* shows the pinning case on the first pit at $v_0 = 0.28$, in Fig. 5, *b* — the case of kink resonance reflection at $v_0 = 0.33$, in Fig. 5, *c* — the case of passing all three impurities at $v_0 = 0.343$, in Fig. 5, *d* — the case of resonant passage or "quasi-tunneling" kink at $v_0 = 0.3426$. The interaction of kink and impurity is inelastic and is accompanied by the emission of free waves and the excitation of localized breather-type waves on impurities.

When the initial velocity of the kink v_0 is less than some critical velocity of passage through three impurities v_{cr}, its pinning is observed on the first, second and third impurities (curves *1*, *2*, *3* in Fig. 3, *b*). From Fig. 3, *b* it can be seen that at the initial moment of time these fluctuations are not harmonic in nature. However, after a long period of time, the oscillations of the oscillators synchronize and become more harmonic.

Pinning scenarios with kink jumping from one "potential pit" to another were also observed

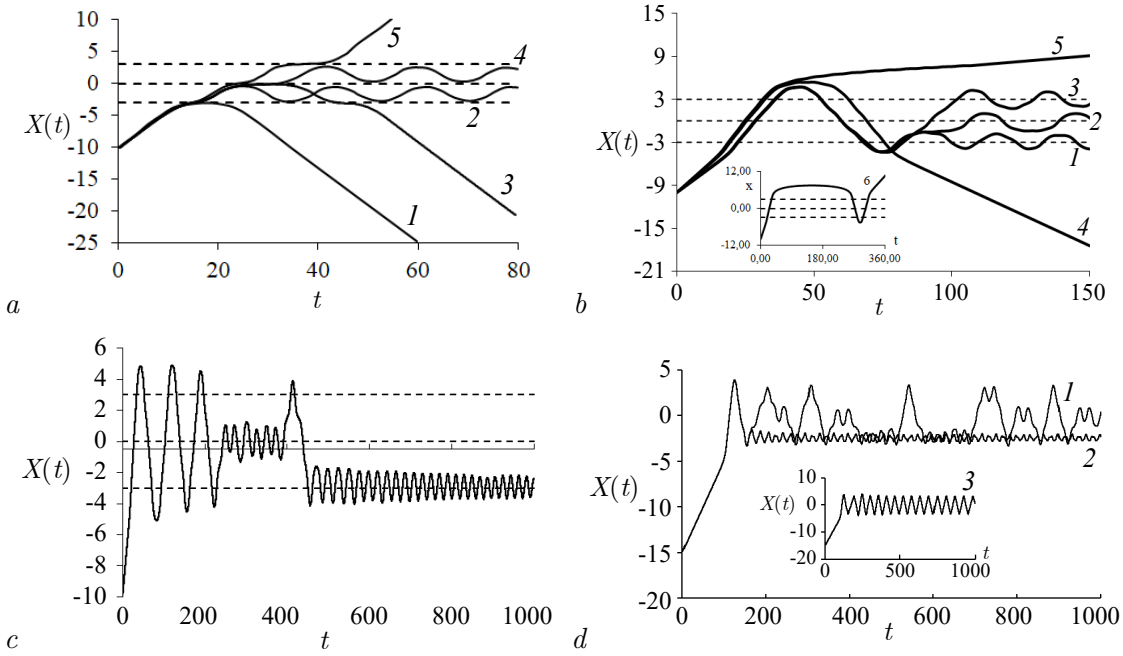

Fig 3. Dependence of the coordinate of the center of kink X on time t. a — The case of a barrier at $W = 1$, $K = 2$, $d = 3$: $v_0 = 0.59$ (line *1*), $v_0 = 0.595$ (*2*), $v_0 = 0.59855$ (*3*), $v_0 = 0.5986$ (*4*), $v_0 = 0.602$ (*5*). b — The case of a well at $W = 1$, $K = 0.5$, $d = 2$: $v_0 = 0.28$ (line *1*), $v_0 = 0.283043899$ (*2*), $v_0 = 0.2849$ (*3*), $v_0 = 0.33$ (*4*), $v_0 = 0.343$ (*5*), $v_0 = 0.3426$ (*6*). c — The case of a well at $d = 2$, $W = 1$, $K = 0.5$, $v_0 = 0.3$. d — The case of a well at $W = 0.5$, $K = 0.5$, $v_0 = 0.1$: $d = 1.52$ (line *1*), $d = 1.55$ (*2*), $d = 1.505$ (*3*)

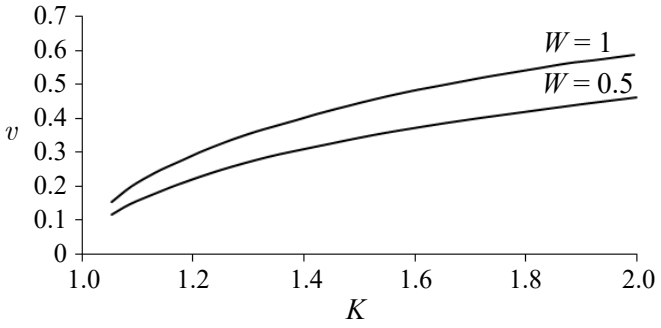

Fig 4. Dependence of the minimum velocity of the kink passage over three impurities on the parameter K

(Fig. 3, *c*). This behavior of the kink is due to the loss of energy for radiation, the excitation of internal degrees of freedom of the kink (pulsation mode), the excitation of localized breather-type oscillations on impurities and their interaction with each other. The oscillation frequencies of the kink on the central and lateral impurities are not equal, although the impurities are the same ($\omega_a = 0.301$, $\omega_b = 0.318$, $\omega_c = 0.301$). As in the case of one and two impurities [27, 28, 31], at certain values of velocities less than v_{cr}, an interesting dynamic effect of resonant reflection of the kink from attracting impurities that are potential wells is observed (curve *4* fig. 3, *b*).

In this case, the kink, after passing through the areas of impurities, stops, then begins to move back and goes in the opposite direction from the initial one at a speed of 0.19. This effect, as in the case of one and two impurities, is resonant in nature, associated with the interaction

of kink with localized breather-type waves originating on impurities. The loss of kinetic energy of the kink to generate breathers and wave radiation is associated with a decrease in its final velocity compared to the initial one.

As in the case of two attracting impurities [29], another resonant effect was observed "quasi-tunneling". In this case, the kink, having a speed less than the minimum required to overcome the areas of the three impurities, passes through them (curve *6* Fig. 3, *b*). With a further increase in the kink speed to a certain value v_{cr} (curve *5* Fig. 3, *b*) it goes on indefinitely. A similar dynamic behavior of the kink was obtained earlier for the case of two impurities [29].

Different scenarios of kink dynamics can be obtained by changing the distance between impurities without changing the initial velocity and parameters of the impurities themselves. For example, for a system with parameters $W = 1$, $K = 0.5$ and an initial velocity of $v_0 = 0.1$, up to $d_1 \approx 1.505$, the kink will fluctuate in the region of all three impurities, that is, the impurities act as one effective (Fig. 1, *b*, curve *4*).

With further increase in d, the dynamics scenarios change (Fig. 3, *d*, curves *1* and *2*). For $d = 1.52$, fluctuations are unstable. The kink jumps between single impurities and effective impurities. Already at $d = 1.55$, king makes only one incomplete oscillation in the area of the effective impurity and is captured by the first impurity. This scenario is similar to the case shown in Fig. 3, *b*, curve *1*.

With a further increase of d to a certain value of $d_2 \approx 2.3$, the nature of the kink fluctuations

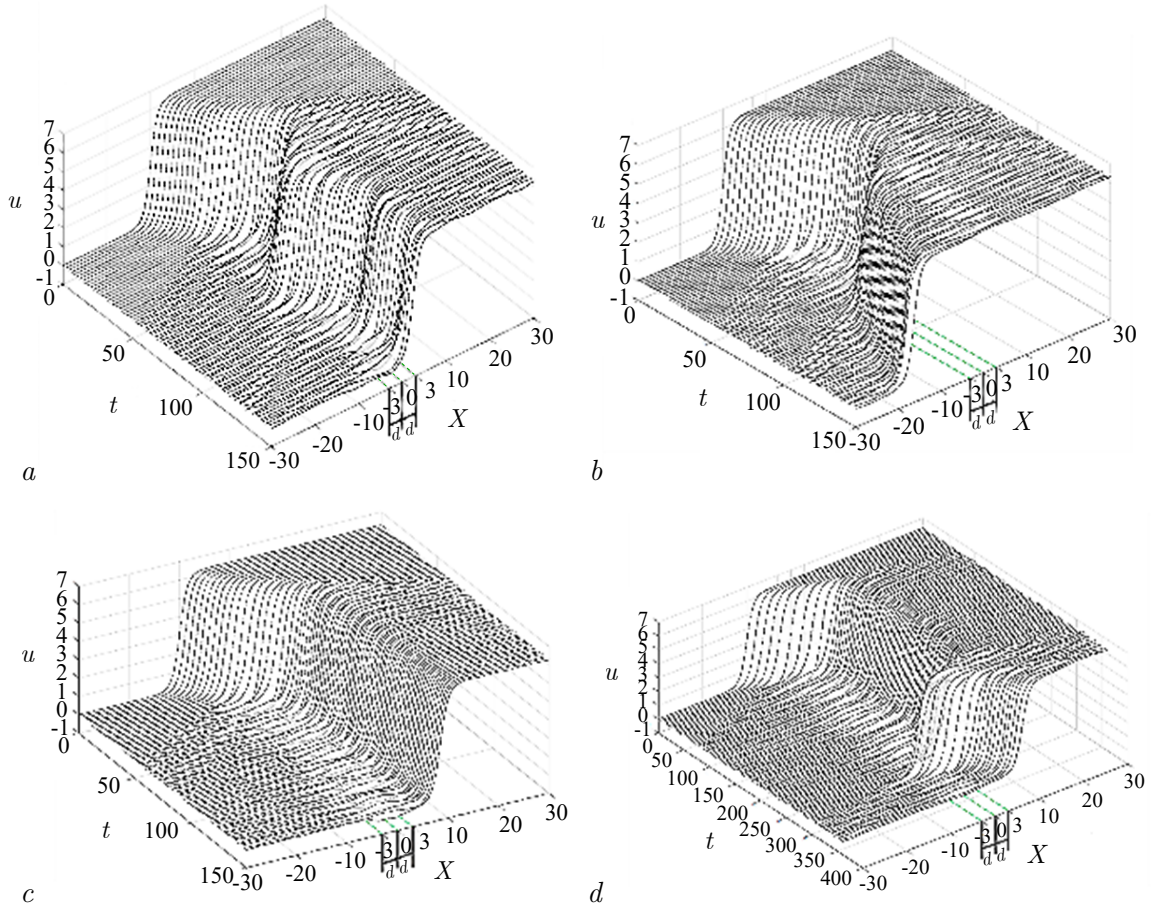

Fig 5. Dependence of $u(X,t)$ at $K = 0.5$, $W = 1$, $d = 2$: *a* — $v_0 = 0.28$, *b* — $v_0 = 0.33$, *c* — $v_0 = 0.343$, *d* — $v_0 = 0.3426$

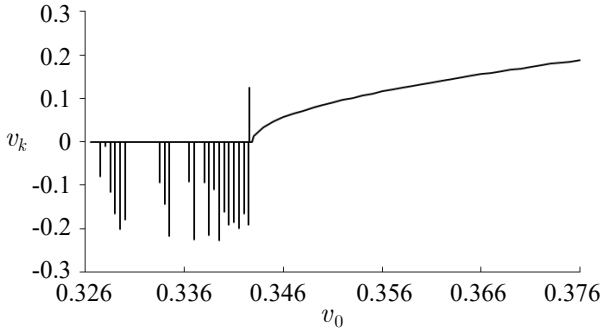

Fig 6. Dependence of the final kink velocity v_k on the initial one v_0 at $W = 1$, $K = 0.5$ and $d = 2$

changes again. If in the area of $1.505 < d < 2.3$ the kink experiences fluctuations in the area of the effective impurity, followed by capture on one of the single ones, then at $2.3 < d < 2.485$ the kink passes through all the impurities and goes to infinity. In the region of $2.485 < d < 3.64$, the collective influence of impurities continues to decrease, transients decrease and the kink is captured by single impurities. In this area, scenarios of kink capture by an impurity without transients appear, however, such scenarios are unstable and disappear with the slightest changes in the distance between the impurities.

In the region of $3.64 < d < 3.8$, the kink does not experience transients and is immediately captured by the third impurity. At $3.8 < d < 5.7$, kink spinning is observed on the second impurity. Starting from $d = 5.8$, the kink is captured by the first impurity. The minimum speed required for a kink to pass through one impurity, in our case, is 0.12. Similar scenarios of kink dynamics can be obtained without changing its velocity and the distance between impurities, but by changing their parameters K and W.

Numerical calculation has shown that the dependence of the final kink velocity on the magnitude of the initial velocity contains many resonant velocities (Fig. 6). These velocities, as in the case of one and two impurities, appear with a certain periodicity. As they approach the critical velocity of passage over the three impurities, their number increases. The vertical line in Fig. 6 corresponds to the "quasi-tunneling" scenario described above.

When the value of v_{cr} is exceeded, the final kink velocity increases non-linearly. The same dependence is typical for the case of one and two impurities [23, 29]. For the case we have considered, $W = 1$, $K = 0.5$, $d = 2$, the formula obtained in [3] for the case of a single impurity

$$v_k^2 = c(v_0^2 - v_{\text{min}}^2), \tag{15}$$

and linking the final kink velocity with the initial one, which has a value greater than v_{cr}, with a coefficient value of $c = 1.47$, well describes the value of the final velocity. Analysis of the results of the numerical experiment shows that this coefficient in our case is a function of the parameters W, K, d and n — the amount of impurities. This dependence can be roughly represented as

$$c_{\text{theor}} = WKdn/2. \tag{16}$$

For example, for the case discussed above, $c_{\text{theory}} = 1.\ 5$ coincides with a fairly high accuracy with the value of $c = 1.47$ obtained numerically.

Conclusion

The article considers the nonlinear dynamics of the kink of the sine-Gordon equation in a model with three identical impurities located at the same distance from each other. All possible

scenarios of kink dynamics were determined and described taking into account resonant effects. For the case of a point impurity described using the delta function, a system of differential equations describing the dynamics of kink and oscillations of waves localized on impurities is obtained using the method of collective variables. It is shown that significant differences are observed in the interaction of kink with a repulsive and attractive admixture. The resonant effects of reflection and passage over impurities are observed only in the case of attracting impurities. The dynamics of the kink in the case of extended impurities was investigated using the numerical finite difference method with an explicit integration scheme. It is established that the found scenarios of kink dynamics for an extended rectangular impurity are qualitatively similar to the scenarios obtained for a point impurity described using the delta function. The analysis of the influence of system parameters and initial velocities on possible scenarios of kink dynamics is carried out. The critical and resonant kink velocities are found as a function of the impurity parameters. It is shown that by changing the distance between impurities, it is possible to effectively control the magnitude of the kink-impurity interaction. Critical values of the distance between impurities are found when three impurities act on the kink as one effective and when impurities act on the kink almost independently of each other.

References

1. Belova TI, Kudryavtsev AE. Solitons and their interactions in classical field theory. Phys. Usp. 1997;40(4):359–386. DOI: 10.1070/PU1997v040n04ABEH000227.
2. Cuevas-Maraver J, Kevrekidis PG, Williams F, editors. The sine-Gordon Model and its Applications: From Pendula and Josephson Junctions to Gravity and High-Energy Physics. Cham: Springer; 2014. 263 p. DOI: 10.1007/978-3-319-06722-3.
3. Braun OM, Kivshar YS. The Frenkel-Kontorova Model: Concepts, Methods, and Applications. Berlin, Heidelberg: Springer; 2004. 472 p. DOI: 10.1007/978-3-662-10331-9.
4. Chevizovich D, Michieletto D, Mvogo A, Zakiryanov F, Zdravković S. A review on nonlinear DNA physics. R. Soc. Open Sci. 2020;7(11):200774. DOI: 10.1098/rsos.200774.
5. Starodub IO, Zolotaryuk Y. Fluxon interaction with the finite-size dipole impurity. Phys. Lett. A. 2019;383(13):1419–1426. DOI: 10.1016/j.physleta.2019.01.051.
6. Kryuchkov SV, Kukhar EI. Nonlinear electromagnetic waves in semi-Dirac nanostructures with superlattice. Eur. Phys. J. B. 2020;93(4):62. DOI: 10.1140/epjb/e2020-100575-4.
7. Kiselev VV, Raskovalov AA, Batalov SV. Nonlinear interaction of domain walls and breathers with a spin-wave field. Chaos, Solitons & Fractals. 2019;127:217–225. DOI: 10.1016/j.chaos.2019.06.013.
8. Ekomasov EG, Nazarov VN, Gumerov AM, Samsonov KY, Murtazin RR. External magnetic field control of the magnetic breather parameters in a three-layer ferromagnetic structure. Letters on Materials. 2020;10(2):141–146 (in Russian). DOI: 10.22226/2410-3535-2020-2-141-146.
9. Delev VA, Nazarov VN, Scaldin OA, Batyrshin ES, Ekomasov EG. Complex dynamics of the cascade of kink–antikink interactions in a linear defect of the electroconvective structure of a nematic liquid qrystal. JETP Letters. 2019;110(9):607–612. DOI: 10.1134/S0021364019210069.
10. Kälbermann G. The sine-Gordon wobble. J. Phys. A: Math. Gen. 2004;37(48):11603–11612. DOI: 10.1088/0305-4470/37/48/006.
11. Ferreira LA, Piette B, Zakrzewski WJ. Wobbles and other kink-breather solutions of the sine-Gordon model. Phys. Rev. E. 2008;77(3):036613. DOI: 10.1103/PhysRevE.77.036613.
12. Dorey P, Gorina A, Perapechka I, Romańczukiewicz T, Shnir Y. Resonance structures in kink-antikink collisions in a deformed sine-Gordon model. Journal of High Energy Physics. 2021;2021(9):145. DOI: 10.1007/JHEP09(2021)145.
13. Fabian AL, Kohl R, Biswas A. Perturbation of topological solitons due to sine-Gordon

equation and its type. Communications in Nonlinear Science and Numerical Simulation. 2009;14(4):1227–1244. DOI: 10.1016/j.cnsns.2008.01.013.
14. Saadatmand D, Dmitriev SV, Borisov DI, Kevrekidis PG. Interaction of sine-Gordon kinks and breathers with a parity-time-symmetric defect. Phys. Rev. E. 2014;90(5):052902. DOI: 10.1103/PhysRevE.90.052902.
15. Kivshar YS, Pelinovsky DE, Cretegny T, Peyrard M. Internal modes of solitary waves. Phys. Rev. Lett. 1998;80(23):5032–5035. DOI: 10.1103/PhysRevLett.80.5032.
16. González JA, Bellorín A, Guerrero LE. Internal modes of sine-Gordon solitons in the presence of spatiotemporal perturbations. Phys. Rev. E. 2002;65(6):065601. DOI: 10.1103/PhysRevE.65.065601.
17. González JA, Bellorín A, García-Ñustes MA, Guerrero LE, Jiménez S, Vázquez L. Arbitrarily large numbers of kink internal modes in inhomogeneous sine-Gordon equations. Phys. Lett. A. 2017;381(24):1995–1998. DOI: 10.1016/j.physleta.2017.03.042.
18. Gomide OML, Guardia M, Seara TM. Critical velocity in kink-defect interaction models: Rigorous results. Journal of Differential Equations. 2020;269(4):3282–3346. DOI: 10.1016/j.jde.2020.02.030.
19. Javidan K. Analytical formulation for soliton-potential dynamics. Phys. Rev. E. 2008;78(4):046607. DOI: 10.1103/PhysRevE.78.046607.
20. Piette B, Zakrzewski WJ. Scattering of sine-Gordon kinks on potential wells. J. Phys. A: Math. Theor. 2007;40(22):5995–6010. DOI: 10.1088/1751-8113/40/22/016.
21. Al-Alawi JH, Zakrzewski WJ. Scattering of topological solitons on barriers and holes of deformed Sine–Gordon models. J. Phys. A: Math. Theor. 2008;41(31):315206. DOI: 10.1088/1751-8113/41/31/315206.
22. Baron HE, Zakrzewski WJ. Collective coordinate approximation to the scattering of solitons in modified NLS and sine-Gordon models. Journal of High Energy Physics. 2016;2016(6):185. DOI: 10.1007/JHEP06(2016)185.
23. Gumerov AM, Ekomasov EG, Murtazin RR, Nazarov VN. Transformation of sine-Gordon solitons in models with variable coefficients and damping. Computational Mathematics and Mathematical Physics. 2015;55(4):628–637. DOI: 10.1134/S096554251504003X.
24. Goodman RH, Haberman R. Interaction of sine-Gordon kinks with defects: the two-bounce resonance. Physica D: Nonlinear Phenomena. 2004;195(3–4):303–323. DOI: 10.1016/j.physd.2004.04.002.
25. Gumerov AM, Ekomasov EG, Zakir'yanov FK, Kudryavtsev RV. Structure and properties of four-kink multisolitons of the sine-Gordon equation. Computational Mathematics and Mathematical Physics. 2014;54(3):491–504. DOI: 10.1134/S0965542514030075.
26. Ekomasov EG, Gumerov AM, Murtazin RR. Interaction of sine-Gordon solitons in the model with attracting impurities. Mathematical Methods in the Applied Sciences. 2016;40(17):6178–6186. DOI: 10.1002/mma.3908.
27. Ekomasov EG, Gumerov AM, Kudryavtsev RV. On the possibility of the observation of the resonance interaction between kinks of the sine-Gordon equation and localized waves in real physical systems. JETP Letters. 2015;101(12):835–839. DOI: 10.1134/S0021364015120061.
28. Ekomasov EG, Gumerov AM, Kudryavtsev RV. Resonance dynamics of kinks in the sine-Gordon model with impurity, external force and damping. Journal of Computational and Applied Mathematics. 2017;312:198–208. DOI: 10.1016/j.cam.2016.04.013.
29. Ekomasov EG, Gumerov AM, Kudryavtsev RV, Dmitriev SV, Nazarov VN. Multisoliton dynamics in the sine-Gordon model with two point impurities. Brazilian Journal of Physics. 2018;48(6):576–584. DOI: 10.1007/s13538-018-0606-4.
30. Gumerov AM, Ekomasov EG, Kudryavtsev RV, Fakhretdinov MI. Excitation of large-amplitude localized nonlinear waves by the interaction of kinks of the sine-Gordon equation with attracting impurity. Russian Journal of Nonlinear Dynamics. 2019;15(1):21–34.

DOI: 10.20537/nd190103.
31. Ekomasov EG, Murtazin RR, Bogomazova OB, Gumerov AM. One-dimensional dynamics of domain walls in two-layer ferromagnet structure with different parameters of magnetic anisotropy and exchange. J. Magn. Magn. Mater. 2013;339:133–137. DOI: 10.1016/j.jmmm.2013.02.042.
32. Ekomasov EG, Murtazin RR, Nazarov VN. Excitation of magnetic inhomogeneities in three-layer ferromagnetic structure with different parameters of the magnetic anisotropy and exchange. J. Magn. Magn. Mater. 2015;385:217–221. DOI: 10.1016/j.jmmm.2015.03.019.
33. Gumerov AM, Ekomasov EG, Kudryavtsev RV. One-dimensional dynamics of magnetic inhomogeneities in a three- and five-layer ferromagnetic structure with different values of the magnetic parameters. J. Phys.: Conf. Ser. 2019;1389:012004. DOI: 10.1088/1742-6596/1389/1/012004.
34. Ekomasov EG, Samsonov KY, Gumerov AM, Kudryavtsev RV. Nonlinear waves of the sine-Gordon equation in the model with three attracting impurities. Izvestiya VUZ. Applied Nonlinear Dynamics. 2022;30(6):749–765. DOI: 10.18500/0869-6632-003011.
35. Magnus K. Schwingungen: Eine Einführung in die theoretische Behandlung von Schwingungsproblemen. 4 Auflage. Wiesbaden: Vieweg+Teubner Verlag; 1961. 252 s. (in German). DOI: 10.1007/978-3-663-10702-6.
36. Faleychik BV. One-Step Methods for the Numerical Solution of the Cauchy Problem. Minsk: Belarusian State University; 2010. 42 p. (in Russian).